African Journal of Basic & Applied Sciences 3 (2): 27-34, 2011
ISSN 2079-2034

A Theoretical Structure Study Nmr of $C_{60}O$ Isomers Through ab Initio Method

[1]Rashid Nizam, [2]S. Mahdi A. Rizvi and [1]Ameer Azam

[1]Department of Applied Physics, Aligarh Muslim University, Aligarh, India
[2]Department of Mechanical Engineering, Aligarh Muslim University, Aligarh, India

Abstract: The NMR spectra of different $C_{60}O$ isomers have been calculated through ab initio method. It has been observed that all the simulated NMR spectra of $C_{60}O$ isomers are almost matching with the available experimental data in literature. The simulated spectrum of each isomer is coming out slightly different from the other two isomers. It is interest tha4 the simulated second isomer of [5, 6] $C_{60}O$ matches the most with the available experimental data in literature. The isomeric structures of $C_{60}O$ are very sensitive to electron correlation treatment with basis set that are employed. So the structure of $C_{60}O$ has been not calculated from semi-empirical methods such as MNDO or AM1 for more accuracy. It is interesting that the isomer epoxide [6, 6] is more stable than the open [5, 6] isomers of $C_{60}O$ during rearrangement from the [6, 6] isomer to the [5, 6] isomer transition still the NMR spectrum of the first simulated of open [5, 6] matching with the most available experimental data. The simulated NMR of the second $C_{60}O$ isomer is also good agreeing with the experimental NMR of $C_{60}O$ with 11% errors.

Key words:

INTRODUCTION

Although the buckminsterfullerene C_{60} is discovered more than two decades ago, yet fullerene properties has grown into an important field in nanotechnology. Fullerenes are also stable molecules just like graphite and diamond, which have an extended solid-state structure, soluble in various organic solvents. This lets for derivatization of fullerene via a variety of functional groups, materialization of unique physical and chemical properties of fullerene derivatives so produced. For example, it was famous that some alkaline metals doped C_{60} reveal superconductivity even at the temperatures higher than 30 K, [1, 2] and unexpected changes in magnetic susceptibility with temperature was also observed for numerous alkali-metal fullerides, [3-6] which was explicated, through theoretical calculations utilizing ab initio and DFT methods, in terms of spin-state transition between different crystalline phases existing in those fullerides. [7] Fullerene monomers can also be modified to dimers via nucleophiles such as cyanide or hydroxide in the solid-state reaction [8] and polymerized fullerenes with three-dimensional structures with hardness surpassing diamond could be fabricated under high pressure and high temperature conditions. [9-11] Besides to the common exohedral fullerene derivatives where atoms or molecules are connected to the ring outside the fullerene cage, it has been shown that small atoms or molecules such as hydrogen could be introduced into the fullerene cage, [12] forming endohedral fullerene complexes with potential purposes in the development of molecular electronic materials.

Although, the demonstration of the diverse aspects of fullerene chemistry plus the importance of employing proper theoretical and experimental methods to understand the structures and properties of fullerene derivatives. The simplest fullerene oxide, $C_{60}O$, is an interesting chemical species. As a simple fullerene derivative, so it can serve as a starting material for more complex fullerene oxides [13, 14] in addition to an important ingredient in the synthesis of a range of chemical compounds. [13-22] Besides it has an improved antioxidant activity [23] along with much shorter lifetime in its triplet state compared to fullerene. [24] Fascinatingly, it was suggested from theoretical calculations that the oxygen atom could also be encapsulated inside the fullerene cage if it acquires enough energy to overcome both the bond formation of exohedral $C_{60}O$ in addition to the potential barrier to endohedral $O@C_{60}$ complex. It was approximated to be about 89 kcal/mol at the B3LYP/3-21G level. [25] The first reported synthesis of $C_{60}O$ by Creegan *et al.* in 1992,[26]

Corresponding Author: Rashid Nizam, Department of Applied Physics, Aligarh Muslim University, Aligarhm, India.
E-mail: - rashid.nizam@gmail.com.

Fig. 1: Schematic view of the C60O configurations corresponding to the [6, 6], transition state and [5,6] position. Oxygen atoms are in red.

the structure and stability of $C_{60}O$ has been the subject of many experimental [24,27-30] with theoretical [31-37] studies as the oxygen can bridge either to the carbon atoms adjacent two six-member rings [6,6] epoxide form) or one five- plus one six-membered ring [5,6] open form). Though it has been primarily found from ^{13}C NMR and IR measurements [26] that $C_{60}O$ should be the epoxide C_{2v} structure with an oxygen atom connecting two six-member rings; later experimental study using fullerene ozonide by Weisman *et al.* [28] confirmed that both the epoxide [6, 6] and open (annulenelike) [5,6] isomeric form can be prepared, depending on how $C_{60}O$ is synthesized. Such as, fullerene ozonide $C_{60}O_3$ can be dissociated into either the [6, 6] form (in the case of thermolysis) or the [5, 6] form (in the case of photolysis).[28] On the other hand, it was found that the open [5,6] structure spontaneously dimerizes to $C_{120}O_2$ in addition to transforms into epoxide form when irradiated.[29] This powerfully advises that the epoxide form is more stable than the oxidoannulene open structure for $C_{60}O$ at room temperature.

In theory, there have been numerous ab initio and semi empirical studies suggesting that the [5,6] isomer is slightly more stable than the [6,6] isomer [30-33] and reorganize between the two isomers involves two transition states and an intermediate state corresponding to local minimum, [31,33] it has to be note down that the methodologies utilized for these studies could not account for the precise electron correlation or basis set effect on the equilibrium geometries and relative stability between the two isomers for this molecule, particularly considering apparently small energy difference between the two isomers predicted from previous studies. It is interestingly that, a couple of molecular dynamics [34, 35] as well as atomic force calculation [36] studies predicted the epoxide [6, 6] form as the more stable species than the open [5, 6] structure. Thus, in apparent of disagreement between a range of theoretical calculation results and experimental findings, it appears necessary to examine this molecule employing more sophisticated methods that should incorporate sufficient electron correlation treatment with large basis set effect as well as investigating vibrational and thermal contributions to the stability of the molecule.

In this paper we systematically examine the effect of electron correlation and basis set as well as vibrational and thermal effect on the relative stability of the [6, 6] and [5, 6] isomers using ab initio Hartree-Fock method.

Computational Details: The simplest structure of $C_{60}O$ molecule model has sixty carbon nuclei reside on a sphere with an oxygen atom connected two carbon atoms. In the paper three $C_{60}O$ molecule models are given as shown figure1. The structure of $C_{60}O$ have two different type of C-C bonds, [6, 6]-bond shared by two hexagons and [5, 6] - bond shared by one pentagon and one hexagon junction i.e. isomers of $C_{60}O$ molecule. The two different C-C bond lengths in C indicate that the ë electrons are not delocalized evenly over all bonds.

CALCULATION

Calculations of NMR shielding tensors have been published from many years [20-23]; these methods are all applicable to calculate the magnetic shielding function of different molecules.

The time-dependent Schrodinger equation is given by

$$H\psi(r,t) = i\frac{\partial}{\partial t}\psi(r,t) \quad (1)$$

It is needed to derive an expression for the current. Differentiating the time-dependent density

$$\rho(r,t) = N \int_{-\infty}^{\infty} dr_2 ... dr_N |\psi(r_1, r_2, ... r_N)|^2 \quad (2)$$

with respect to the time coordinate gives together with Eq. (1) the continuity equation

$$\frac{\partial}{\partial t}\rho(r,t) = -\nabla J(r,t) \quad (3)$$

where $J(r,t)$ is the flux, or the probability current

$$J(r,t) = \frac{1}{2i} v N \int_{-\infty}^{\infty} dr_2 ... dr_N |\left(\psi^* \nabla \psi - \nabla \psi \psi^*\right) \quad (4)$$

When the wave function is real, then the system is independent of time so the current must vanish. As eqn. (3) represents a conservation law i.e. a change in the density in some region must be compensated by flux in or out of that region. The magnetic field is initiated into the quantum mechanical framework through minimal substitution of the magnetic vector potential, A, into the kinetic energy operator

$$p \to \pi = P + \frac{e}{c} A \quad (5)$$

where $p = -i\nabla$, c is the speed of light (in atomic units c = 137.035987) and e is the electron charge. It is feasible to explain that this gives the correct form for the Hamiltonian by considering the Lagrangian for the Lorentz force of an electron in an electromagnetic field [30].

The interested magnetic vector potential of consists of two contributions, $A = A^B + A^m_i$. The first term express a uniform, time-independent external magnetic field.

$$A^B(r) \frac{1}{2} B \times (r - R_o) \quad (6)$$

where R_o is the chosen as the magnetic field origin and the second term is due to the magnetic moments of the nuclei

$$A^{m_1}(r) = \sum_I m_1 \times \frac{r - R_1}{|r - R_1|^3} \quad (7)$$

where m_I is the magnetic moment of the I^{th} nucleus with R_I the nuclear position vector.

The current density $\vec{j}(\vec{r})$ of a fullerene derivative molecule in a stationary external magnetic field $\vec{B}_{ext}$ in the electronic ground state with the corresponding wave function is given by

$$\vec{j}(\vec{r}) = \frac{i}{2}\left[\overline{\nabla}\psi_0^* \psi_0 - \psi_0^* \left(\overline{\nabla}\psi_0\right)\right] - \frac{1}{c}\vec{A}\psi_0^* \psi_0 \quad (8)$$

where $\vec{A}$ is the vector potential of the external magnetic field. The induced field $\vec{B}_{ind}$ at any position $\vec{r}_k$ of a molecule in an external magnetic field $\vec{B}_{ext}$ can be computed using Biot-Savart's law.

$$\vec{B}_{ind}\left(\vec{r}_k\right) \frac{1}{c} \int \frac{\vec{j}(\vec{r}) \times \vec{r}_k}{r_k^3} d^3 r \quad (9)$$

Alternatively to the induced field, a tensorial shielding function $\vec{\vec{\sigma}}(\vec{r}_k)\left(\vec{\vec{\sigma}} \leftrightarrow \sigma_{a\beta}\right)$ may bring in to explain the response of the electronic system in a molecule to the external magnetic field

$$\left(\vec{B}_{ind}\right)_a = -\sum_{\beta-1}^{3} \sigma_{a\beta} \left(\vec{B}_{exd}\right)_\beta \quad (10)$$

This shielding function works just the generalization of the shielding tensor in NMR spectroscopy, where the induced field, respectively, the shielding field, is needed only at a few specific positions of the nuclei in space.

$$\vec{H} = \sum_{k=1}^{N} \left[\frac{\vec{p}_k^2}{2} - \frac{1}{2c} A.\vec{p}_k^2 + \frac{1}{2c^2} \vec{A}^2 \right] + V \quad (11)$$

Where V represents for the electron nucleus with electron-electron interaction potential and $\vec{P}$ is the momentum operator respectively. $\vec{A}$ is the vector potential of the external magnetic field, for which the Coulomb gauge is taken.

$$\vec{j}(\vec{r}) = \frac{1}{2}\left(\vec{B} \times \vec{r}\right) \quad (12)$$

Moreover, it has been considered that $\vec{\nabla}.\vec{A} = 0$. Thinking of only linear terms in the magnetic field ("weak perturbation"), the perturbation operator of the external magnetic field $\vec{H}\left(\vec{H} = \vec{H}^{(0)} + \vec{H}^{(1)}\right)$ is given by

$$\vec{H} = -\left(\vec{B}_{ext} \times \vec{r}\right).\vec{\nabla} = \frac{1}{2c} \vec{B}_{exd} \vec{L} \quad (13)$$

where $\vec{L}$ denotes the angular momentum operator. The current density $\vec{j}(\vec{r})$ can be expanded in a Taylor series in $\vec{B}_{ext}$.

$$\vec{j}(\vec{r}) = \vec{j}^{(0)}(\vec{r}) + \vec{j}^{(1)}(\vec{r}) + \ldots. \quad (14)$$

$$\vec{j}^{(1)}(\vec{r}) = \vec{B}_{ext}\vec{\vec{j}}^{(1)}(\vec{r}) \quad (15)$$

with $\left(\vec{\vec{j}}^{(1)}(\vec{r})\right)_{a\beta} = \frac{\partial\left(\vec{j}(\vec{r})\right)_a}{\partial\left(\vec{B}\right)_\beta}$

where $\vec{j}^{(1)}(\vec{r})$ is the current density in a molecule with no external magnetic field. It finishes for molecules without a permanent magnetic moment. With a corresponding expansion of the wave function:

$$?_j = ?_j^{(0)} + i\vec{B}_{ext}.?_j^{(1)} + \ldots \quad (16)$$

the current density up to linear terms in the magnetic field might then be written as:

$$\vec{B}_{ext}.\vec{\vec{j}}^{(1)}(\vec{r}) = \frac{1}{2}\left\{\vec{B}_{ext}.\left[\begin{array}{c} ?_0^{(0)}\left(\vec{\nabla}.\vec{\psi}_0^{(1)}\right) - \vec{\psi}_0^{(1)}\cdot \\ \left[\vec{\nabla}?_0^{(0)} - \frac{1}{c}\vec{A}\left|?_0^{(0)}\right|^2\right] \end{array}\right]\right\} \quad (17)$$

By only these linear terms in Biot-Savart's ,aw, one obtains for the shielding function:

$$\vec{\vec{\sigma}}(\vec{r})\frac{1}{2}\left\langle ?_0^{(0)}\left|\frac{\left(\vec{r}.\vec{r}_k\right)\vec{\vec{I}} - \vec{r}_k \otimes \vec{r}}{r_k^3}\right|?_0^{(0)}\right\rangle - \frac{2}{c}\left\langle ?_0^{(0)}\left|\frac{\vec{L}}{r_k^3}\right|\vec{\psi}_0^{(1)}\right\rangle \quad (18)$$

Where $\vec{\vec{I}}$ denotes the identity matrix. As for the NMR shielding tensors, the first term is called the diamagnetic contribution to $\vec{\vec{\sigma}}$, whereas the second term is called the paramagnetic contribution.

The first-order perturbed wave function $\vec{\psi}_0^{(1)}$ is traditionally expanded in terms of excited states of the unperturbed system

$$\vec{\psi}_0^{(1)} = \sum_{n\neq 0}\vec{C}_n^{(1)}\psi_n^{(0)} \quad (19)$$

This directs to the same expressions as originally derived for the NMR shielding tensors by Ramsey, [24] when $\vec{r}_k$ is restricted to the nuclear positions $\vec{r}_k = R_k$

$$\vec{\vec{\sigma}}(\vec{r})\frac{1}{2}\left\langle ?_0^{(0)}\left|\frac{\left(\vec{r}.\vec{r}_k\right)\vec{\vec{I}} - \vec{r}_k \otimes \vec{r}}{r_k^3}\right|?_0^{(0)}\right\rangle - \frac{2}{c}\sum_{n\neq 0}\frac{1}{E_n - E_0}\left\langle ?_0^{(0)}\left|\frac{\vec{L}}{r_k^3}\right|\vec{\psi}_0^{(1)}\right\rangle \otimes \left\langle ?_0^{(0)}\left|\vec{L}\right|?_0^{(0)}\right\rangle \quad (20)$$

Computations of the shielding function using eqn. (20) would require the knowledge of the complete set of the solutions of the unperturbed (without external magnetic field) many-particle Schrodinger equation $?_0^{(0)}, ?_1^{(0)}, ?_2^{(0)}$ ... with the corresponding energies $E_0^{(0)}, E_1^{(0)}, E_2^{(0)}$..... Although, concerning the Coulomb interactions between the electrons, only approximate solutions of the Schrodinger equation can be obtained in principle. Within the Hamiltonian of eqn. (22), the magnetic field acts only in the kinetic energy part. Therefore, one might expect that the shielding function can simply be calculated by application of eqn (20), just by using approximate solutions for $?_0^{(0)}, ?_1^{(0)}, ?_2^{(0)}$ .... and $E_0^{(0)}, E_1^{(0)}, E_2^{(0)}$..... However, even in the single determinant (Slater determinant) ansatz for the wave function (HF), it turns out that the problem is more involved. Within HF theory, the single particle wave functions (orbitals) Ψ_j of the Slater determinant are solutions of single particle-like equations (HF equations)

$$\vec{F}\psi_j = \in_j \psi_j \quad (21)$$

The Fock operator, $\vec{F}$, the orbitals, Ψ_j and the orbital energies, $\in_j$, are also be expanded in a Taylor series similar manner as in eqn (7) :

$$\begin{aligned} ?_j &= ?_j^{(0)} + i\vec{B}_{ext}.?_j^{(1)} + \ldots \\ \in_j &= \in_j^{(0)} + i\vec{B}_{ext}.\in_j^{(1)} + \ldots \\ \vec{F}_j &= \vec{F}_j^{(0)} + i\vec{B}_{ext}.\vec{F}_j^{(1)} + \ldots \end{aligned} \quad (22)$$

$\vec{F}^{(0)}$ is the Fock operator without an external magnetic field.

$$\vec{F}^{(0)} = \frac{\vec{P}^2}{2} + V_{ext} + \sum_{j=1}^{N_{occ}}\left(2J_j^{(0)} - K_j^{(0)}\right) \quad (23)$$

where V_{ext} stands for the scalar external potential (electron nucleus potential) as well as $J_j^{(0)}$ and $K_j^{(0)}$ are the usual

Coulomb and exchange expressions, respectively. The first-order perturbed Fock operator $\vec{F}^{(1)}$ is, however, not only given by $\vec{H}^{(1)}$ (eqn. 6). There is no first-order correction to *Jj* but there has to be considered one in the exchange part K_j

$$\vec{F}^{(1)} = \vec{B}_{ext.}\vec{H}^{(1)} - \sum_{j=1}^{N_{occ}} \vec{K}_j^{(1)} \tag{24}$$

$$\vec{K}_j^{(1)} = \int \left[\vec{\psi}_j^{(1)}(\vec{r})\psi_j^{(0)}(\vec{r}') - \psi_j^{(0)}(\vec{r})\vec{\psi}_j^{(1)}(\vec{r}') \right] \frac{1}{|\vec{r}-\vec{r}'|} \psi(\vec{r}')\, d^3r' \tag{25}$$

Inserting expansions (21) into eqn. (21), one can obtains up to first order a set of linear equations, which has to be solved successively

$$\left(\vec{h}^{(0)} - \in_j^{(0)}\right)\psi_j^{(0)} = 0 \tag{26}$$

$$i\left(\vec{h}^{(0)} - \in_j^{(0)}\right)\vec{B}_{ext.}\vec{F}_j^{(1)} = \left[\vec{B}_{ext.}\left(\vec{\in}_j^{(1)} - \vec{F}^{(1)}\right)\right]\psi_j^{(0)} \tag{27}$$

Because of the exchange part, the first order perturbed eqn. (8) has to be solved iteratively coupled hartree fock method. [25]

RESULT & DISCUSSIONS

Despite the high symmetry of the $C_{60}O$ molecule, the eigenvectors are, in general, somewhat difficult to visualize. The fullerenes derivative ($C_{60}O$) has 177 degree of freedom. Starting with 177 total degrees of freedom for an isolated $C_{60}O$ molecule and subtracting the six degrees of freedom corresponding to three translations and three rotations, results in 171 vibrational degrees of freedom. The rotational constants in x, y and z axis in the fullerenes derivative ($C_{60}O$) is 0.09, 0.08 and 0.08 (GHz) respectively. The $C_{60}O$ has 305 symmetry adapted basis functions, 915 primitive gaussians, 305 cartesian basis functions, 184 alpha electrons and 184 beta electrons with the nuclear repulsion energy 9190.52 Hartrees. The fullerenes derivative ($C_{60}O$) has done SCF E (RHF) = -2317.13 A.U. after 128 cycles with convergence density matrix= 0.5915D-08.

For ordinary NMR experiment of any C_{60} molecules, the distribution of the ^{12}C to ^{13}C isotopes is in proportion to 75 to 25 percent. Approximately more than half of the molecules in C_{60} samples experiment are $^{12}C_{60}$ molecules, which do not give NMR spectrum. Although the isotope effects discussed above are expected to affect the line intensities of the rotational and rotational-vibrational modes significantly in ordinary C_{60} samples at very low temperatures.

In each model of $C_{60}O$, ^{13}C and ^{17}O are considered to evaluate the total NMR effect on $C_{60}O$ sample. The simulated ^{13}C NMR spectra of $C_{60}O$ contain sixty one lines in each model. In $^{13}C_{60}O$, each ^{13}C atom has a nuclear spin $\varphi = 1/2$ and each molecule thus has 2^{61} nuclear spin states, with φ_{tot} values ranging from $\varphi_{tot} = 0$ to $\varphi_{tot} = 31$. The decomposition of 2^{61} nuclear spin states into irreducible representations of all possible φ_{tot} states has been examined by Harter and Reimer [37], noting that the totally anti-symmetric states of $^{13}C_{60}$ belong to the A_g irreducible representation of I_h, because all operations of I_h are even permutations and the totally anti-symmetric wave function does not change sign under even permutations. Thus the statistical weight for each irreducible representation of I_h for all 2^{61}states of $^{13}C_{60}O$ is well approximated by the dimension of the irreducible representation. The NMR observed peaks and simulated peaks of each model are given below. The number in the bracket represents the number of NMR peaks obtaining at particular frequency. The best ^{13}C NMR spectrum of the first [5, 6] isomer $C_{60}O$ is matching with experimental ^{13}C NMR data.

The observed NMR peaks of $C_{60}O$ [58] are 140.50(1), 141.80(2), 142.07(3), 142.22(4), 142.41(5), 143.0(6), 143.01(7), 143.58(8), 143.97(9), 144.41(10), 144.46(11), 145.15(12), 145.28(13), 145.37(14), 145.45(15) as shown in fig.5.

In detail, the calculated shifts for the first isomer are as shown in fig. 2 and follows (in ppm.): 120.75 (1), 120.77 (2), 120.84 (3), 120.90 (4), 122.54 (5), 122.60 (6), 122.61 (7), 122.62 (8), 122.81 (9), 122.89 (10), 122.91 (11), 123.01 (12), 123.09 (13), 123.13 (14), 123.24 (15), 123.25 (16), 123.26 (17), 123.30 (18), 123.31 (19), 123.33 (20), 123.34 (21), 123.40 (22), 123.41 (23), 123.51 (24), 123.53 (25), 123.53 (26), 123.85 (27), 124.05 (28), 124.06 (29), 124.10 (30), 124.12 (31), 124.14 (32), 124.14 (33), 124.17 (34), 124.20 (35), 124.28 (36), 124.32 (37), 124.33 (38), 124.34 (39), 124.34 (40), 124.45 (41), 124.50 (42), 124.64 (43), 124.71 (44), 124.76 (45), 124.82 (46), 124.83 (47), 124.84 (48), 124.86 (49), 124.87(50), 125.04 (51), 125.13 (52), 125.21 (53), 125.30 (54), 126.34 (55), 126.56 (56), 126.58 (57), 126.65 (58), 193.90 (59), 194.1 (60), 391.91 (61)

In detail, the calculated shifts for the second isomer are as shown in fig. 3 and follows (in ppm.): 116.14 (1), 119.41 (2), 119.49 (3), 120.81 (4), 121.17 (5), 121.46 (6), 121.59 (7), 121.95 (8), 122.05 (9), 122.25 (10), 122.34 (11),

122.65 (12), 122.96 (13), 122.96 (14), 122.98 (15), 122.99 (16), 123.01 (17), 123.06 (18), 123.06 (19), 123.08 (20), 123.14 (21), 123.21 (22), 123.28 (23), 123.37 (24), 123.69 (25), 123.83 (26), 123.85 (27), 123.96 (28), 124.07 (29), 124.21 (30), 124.29 (31), 124.36 (32), 124.58(33), 124.71 (34), 124.80 (35), 125.11 (36), 125.19 (37), 125.55 (38), 124.73 (39), 125.85 (40), 126.51 (41), 126.59 (42), 126.65 (43), 126.69 (44), 126.78 (45), 126.88 (46), 128.25 (47), 128.30 (48), 128.48 (49), 128.52(50), 128.69 (51), 128.88 (52), 130.11 (53), 130.19 (54), 130.77 (55), 134.11 (56), 137.95 (57), 138.33 (58), 194.55 (59), 194.68 (60), 353.63 (61)

In detail, the calculated shifts for the third isomer are as shown in fig. 4 and follows (in ppm.): 115.95 (1), 119.39 (2), 119.69 (3), 121.08 (4), 121.10 (5), 121.32 (6), 121.45 (7), 122.19 (8), 122.19 (9), 122.25 (10), 122.21 (11), 122.63 (12), 122.95 (13), 122.95 (14), 123.02 (15), 123.02 (16), 123.02 (17), 123.04 (18), 123.07 (19), 123.07 (20), 123.09 (21), 123.12 (22), 123.42 (23), 123.61 (24), 123.62 (25), 123.80 (26), 123.85 (27), 123.90 (28), 123.99 (29), 124.31 (30), 124.45 (31), 124.48 (32), 124.55 (33), 124.65 (34), 124.86 (35), 124.90 (36), 125.28 (37), 125.62 (38), 125.72 (39), 126.05 (40), 126.49 (41), 126.59 (42), 126.72 (43), 126.75 (44), 126.79 (45), 126.89 (46), 128.15 (47), 128.21 (48), 128.42 (49), 128.62 (50), 129.22 (51), 130.30 (52), 130.39 (53), 130.40 (54), 133.74 (55), 133.87 (56), 137.89 (57), 138.59 (58), 194.55 (59), 194.60 (60), 353.29 (61)

The average observed [38] NMR of $C_{60}O$ is at 142 ppm which is nearest the simulated NMR of the first isomer [6, 5]. Mostly the NMR peaks of the first isomer [6, 5] are crowded at 125 ppm that when compared with the observed NMR data peak gives 11% error. The error may be due to two reasons. Firstly the experimental sample $^{13}C_{60}O$ might not possess all ^{13}C and ^{17}O during the NMR experiment. Thus obtained fifteen peaks instead

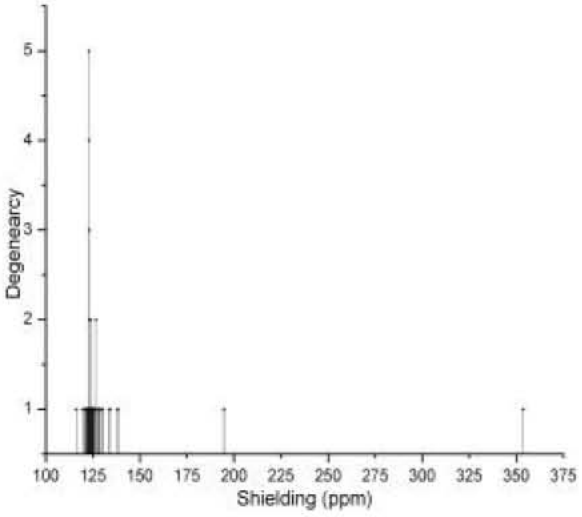

Fig. 2: For NMR Fullerene oxide [6, 6]

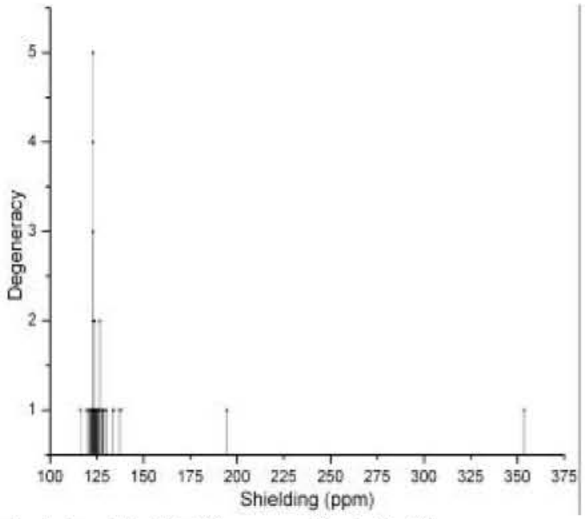

Fig. 3: For NMR Fullerene oxide_1 [6, 5]

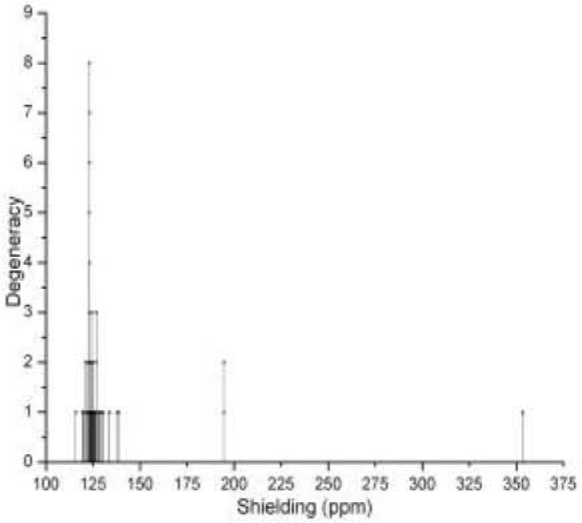

Fig. 4: For NMR Fullerene oxide_2 [6, 5]

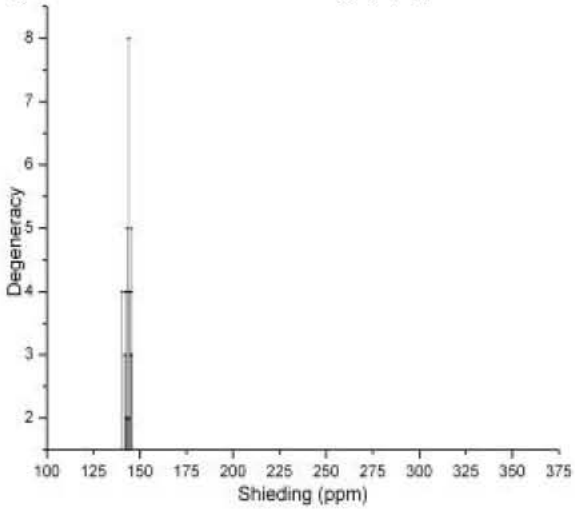

Fig. 5: For NMR experimental data of Fullerene oxide

of six one peaks. Secondly slightly changes distortion occurs in many bond lengths with bond angles among different atoms of $C_{60}O$ during $C_{60}O$ formation. While each $^{13}C_{60}O$ model, the bond length and bond angle are taken ideals expect in two carbon atoms where oxygen atom attached get changed.

CONCLUSION

The isomeric structures of $C_{60}O$ are very sensitive to electron correlation treatment with basis set that are employed. As the structure calculated from semi-empirical methods such as MNDO or AM1 are not very much accurately calculated. So the proper electron correlation level and basis set play an important role in calculating the accurate structure through ab initio method. It is interesting to note that although the isomer structure [6,6] of $C_{60}O$ more stable than the other two isomer [5,6] structure of $C_{60}O$ yet the simulated NMR of first isomer $C_{60}O$ [5,6] matching with the experimental NMR peaks.

REFERENCES

1. Ganin, A.Y., Y. Takabayashi, Y.Z. Khimyak1, S. Margadonna, A. Tamai, M.J. Rosseinskyl and K. Prassides, 2008. Bulk superconductivity at 38K in a molecular system, Nature, 7: 367.
2. Tanigaki, K., T.W. Ebbesen, S. Saito, J. Mizuki, J.S. Tsai, Y. Kubo and S. Kuroshima, 1991. Superconductivity at 33 K in $Cs_xRb_yC_{60}$, Nature, 352: 222.
3. Tycko, R., G. Dabbagh, D.W. Murphy, Q. Zhu, J.E. Fischer, 1993. Electronic properties and phase transitions of RbC_{60} and CsC_{60} Investigation by NMR spectroscopy, Phys. Rev. B., 48: 9097.
4. Chauvet, O., G. Oszlanyi, L. Forro, P.W. Stephens, M. Tegze, G. Faigel and A. Janossy, 1994. Quasi-one-dimensional electronic structure in orthorhombic RbC60, Phys. Rev. Lett., 72: 2721.
5. Oszlanyi, G., G. Bortel, G. Faigel, M. Tegze, L. Granasy, S. Pekker, P. W. Stephens and L. Forro, 1995. Dimerization in KC_{60} and RbC_{60} , Phys. Rev. B., 51: 12228.
6. Bommeli, F., L. Degiorgi, P. Wachter, A. Legeza, A. Janossy, G. Oszlanyi, Chauvet and O.L. Forro, 1995. Metallic conductivity and metal-insulator transition in $(AC_{60})n$ (A=K, Rb and Cs) linear polymer fullerides Phys. Rev. B ., 51: 14794.
7. Kim, K.S., J.M. Park, J. Kim, S.B. Suh, P. Tarakeshwar, K.H Lee and S.S. Park, 2000. Dimer to Monomer Phase Transition in Alkali-Metal Fullerides: Magnetic Susceptibility Changes, Phys. Rev. Lett., 84: 2425.
8. Komatsu, K., K. Fujiwara, T. Tanaka, Y. Murata, The fullerene dimer C120 and related carbon allotropes, Carbon, 38: 1529.
9. Blank, V.D., S.G. Buga, N.R. Serebryanaya, V.N. Denisov, G.A. Dubitsky, A.N. Ivlev, B.N. Mavrin and M.Y. Popov, 1995. Ultrahard and superhard carbon phases produced from C60 by heating at high pressure: structural and Raman studies, Phys. Lett. A., 205: 208.
10. Serebryanaya, N.R., V.D. Blank, V.A. Ivdenko, L.A. Chernozatonskii, 2001. Pressure-induced superhard phase of C_{60}, Solid State Commun., 118: 183.
11. Talyzin, A.V., L.S. Dubrovinsky, M. Oden, T. Le Bihan, U. Jansson, 2002. In situ x-ray diffraction study of C60 polymerization at high pressure and temperature, Phys. Rev. B., 66: 165409.
12. Hummelen, J.C., M. Prato, F. Wudl, There Is a Hole in My Bucky, J. Am. Chem. Soc., 117: 7003.
13. Smith, A.B., III, H. Tokuyama, R.M. Strongin, G.T. Furst, W.J. Romanow, B.T. Chait, U.A. Mirza and I. Haller, 1995. Synthesis of Oxo- and Methylene-Bridged C_{60} Dimers the First Well-Characterized Species Containing Fullerene-Fullerene Bonds, J. Am. Chem. Soc., 117: 9395.
14. Deng, J.P., C.Y. Mou and C.C. Han, 1996. $C_{180}O_2$ a V-shaped fullerene trimer, J. Chem. Phys. Lett., 256: 96.
15. Deng, J.P., C.Y. Mou and C.C. Han, 1995. Electrospray and Laser Desorption Ionization Studies of $C_{60}O$ and Isomers of $C_{60}O_2$ J. Phys. Chem., 99: 14907.
16. Gromova, A., S. Ballenwega, S. Giesab, S. Lebedkinc, W.E. Hulld and W. Krätschmera, 1997. Preparation and characterisation of C_{119}, Chem. Phy. Lett., 267(5-6): 460-466.
17. Kumar, S. and R.W. Murray, 1980. An intramolecular oxenoid oxidation , Tetrahedron Lett., pp: 4781-4782.
18. Beck, R.D., G. Brauchle, C. Stoermer and M.M. Kappes, 1995. Synthesis of $C_{120}O$ A new dimeric [60] fullerene derivative, J. Chem. Phys., 102: 540.
19. Balch, A.L., D.A. Costa and M.M. Olmstead, 1996. Developing Reagents To Orient Fullerene Derivatives. Formation and Structural Characterization of (eta(2)-$C_{(60)}O$)Ir (CO) Cl(As($C_{(6)}H_{(5)}$)$_{(3)}$)$_{(2)}$. Inorg. Chem., 35: 458.

20. Fedurco, M., D.A. Costa, A.L. Balch and W.R. Favcelt, 1995. Angew. Chem. Int. Ed. Engl., 34: 194.
21. Tajima, Y. and K. Takeuchi, 2002. Discovery of $C_{60}O_3$ Isomer Having C_3V Symmetry, J. Org. Chem., 67: 1696.
22. Balch, A.L., D.A. Costa, J.W. Lee, B.C. Noll and M.M. Olmstead Transition metal fullerene chemistry: 1999. The route from structural studies of exohedral adducts to the formation of redox active films, Inorg. Chem., 33: 2071.
23. Matsubayashi, K., T. Goto, K. Togaya, K. Kokubo, T. Oshima, 2008. Effects of Pin-up Oxygen on [60] Fullerene for Enhanced Antioxidant Activity, Nanoscale Res. Lett., 3: 237.
24. Benedetto, A.F. and R.B.Weisman, 1999. Unusual triplet state relaxation in C_{60} oxide, Chem. Phys. Lett., 310: 25.
25. Park, J.M. T. Tarakeshwar, K.S. Kim and T. Clark, 2002. Nature of the interaction of paramagnetic atoms ($A=^4N,^4P,^3O,^3S$) with ð systems and C_{60}: A theoretical investigation of $A\bullet\bullet\bullet C_6H_6$ and endohedral fullerenes AC_{60}, J. Chem. Phys., 116: 10684.
26. Creegan, K.M., J.L. Robbins, W.K. Robbins, J.M. Millar, R.D. Sherwood, P.J. Tindall, D.M. Cox, A.B. III Smith, J.P. Jr. McCauley, D.R. Jones and R.T. Gallagher, 1992. J. Am. Chem. Soc., 114: 1103.
27. Heymann, D., S.M. Bachilo, R.B Weisman, F. Cataldo, R.H. Fokkens, N.N.M. Nibbering, R.D. Vis and L.P.F. 2000. Chibante, J. Am. Chem. Soc., 122: 11437.
28. Weisman, R.B., D. Heymann and S.M. Bachilo, 2001. Synthesis and Characterization of the Missing Oxide of C60 [5,6]-Open C60O, J. Am. Chem. Soc. 123: 9720.
29. Tsyboulski, D., D. Heymann, S.M. Bachilo and R.B. Weisman, 2002. Abstract Volume of the 201st Meeting of the Electrochemical Society; Philadelphia, pp: 12-17.
30. Raghavachari, K., 1992. Structure of $C_{60}O$: unexpected ground state geometry, Chem. Phys. Lett.,pp: 221-224.
31. Raghavachari, K. and C. Sosa, 1993. Fullerene derivatives. Comparative theoretical study of $C_{60}O$ and $C_{60}CH_2$, Chem. Phys. Lett., pp: 223-228.
32. Wang, B.C., L. Chen, H.W. Wang and Y.M. Chou, 1999. Spherical shape of the goldberg type giant fullerenes Theochem, pp: 2448-2449.
33. Xu, X., Z. Shang, Li Ruifang, Z. Cai and X. Zhao, 2002. Theoretical studies on the mechanism of 1,3-dipolar cycloaddition of methyl azide to [50] fullerene, J. Phys. Chem., 106: 9284.
34. Menon, M. and K.R. Subbaswamy, 1993. Structure and properties of C60 dimers by generalized tight-binding molecular dynamics, Chem. Phys. Lett., 201: 321.
35. Wang, B.C., L. Chen, K.J. Lee and C.Y. Cheng, 1999. Semi empirical molecular dynamics studies of C_{60}/C_{70} fullerene oxides $C_{60}O$, $C_{60}O_2$ and $C_{70}O$, Theo Chem., 469: 127.
36. Batirev, I.G., K.H. Lee and J.A. Leiro, 2000. Atomic structure and chemical bonding of boro and azafullerene dumb-bells, Chem. Phys. Lett., pp: 695-699.
37. Snoke, D.W., M. Cardona, S. Sanguinetti and G. Benedek, 1993. Comparison of bond character in hydrocarbons and fullerenes, Solid State Commun. Phy. Rev. B., 87: 121.
38. Kathleen, M.C., J.L. Robbins, W.K. Robbins, J.M. Millar, R.D. Sherwood, P.J. Tindall, D.M. Cox, J.P. M Jr. and D.R. Jones, 1992. Synthesis and characterization of C60O, the first fullerene epoxide, J. Am. Chem. SOC., 114: 1103-1105.